

The phospholipase A₁ activity of lysophospholipase A-I links platelet activation to LPA production during blood coagulation[§]

Alyssa L. Bolen,* Anjaparavanda P. Naren,* Sunitha Yarlagadda,* Sarka Beranova-Giorgianni,[†] Li Chen,[†] Derek Norman,[§] Daniel L. Baker,[§] Meng M. Rowland,** Michael D. Best,** Takamitsu Sano,^{1,††} Tamotsu Tsukahara,^{2,*††} Karoly Liliom,*^{§§} Yasuyuki Igarashi,^{††} and Gabor Tigyi^{3,*}

Departments of Physiology* and Pharmaceutical Sciences,[†] University of Tennessee Health Science Center, Memphis, TN; Department of Chemistry,[§] University of Memphis, Memphis, TN; Department of Chemistry,** University of Tennessee, Knoxville, TN; Frontier Research Center for Post-Genome Science and Technology,^{††} Faculty of Advanced Life Science, Hokkaido University, Sapporo, Japan; and Institute of Enzymology,^{§§} Biological Research Center of the Hungarian Academy of Sciences, Budapest, Hungary

Abstract Platelet activation initiates an upsurge in polyunsaturated (18:2 and 20:4) lysophosphatidic acid (LPA) production. The biochemical pathway(s) responsible for LPA production during blood clotting are not yet fully understood. Here we describe the purification of a phospholipase A₁ (PLA₁) from thrombin-activated human platelets using sequential chromatographic steps followed by fluorophosphonate (FP)-biotin affinity labeling and proteomics characterization that identified acyl-protein thioesterase 1 (APT1), also known as lysophospholipase A-I (LYPLA-I; accession code O75608) as a novel PLA₁. Addition of this recombinant PLA₁ significantly increased the production of *sn*-2-esterified polyunsaturated LPCs and the corresponding LPAs in plasma. We examined the regioisomeric preference of lysophospholipase D/autotaxin (ATX), which is the subsequent step in LPA production. To prevent acyl migration, ether-linked regioisomers of oleyl-*sn*-glycero-3-phosphocholine (lyso-PAF) were synthesized. ATX preferred the *sn*-1 to the *sn*-2 regioisomer of lyso-PAF. We propose the following LPA production pathway in blood: 1) Activated platelets release PLA₁; 2) PLA₁ generates a pool of *sn*-2 lysophospholipids; 3) These newly generated *sn*-2 lysophospholipids undergo acyl migration to yield *sn*-1 lysophospholipids, which are the preferred substrates of ATX; and 4) ATX cleaves the *sn*-1 lysophospholipids to generate *sn*-1 LPA species containing predominantly 18:2 and 20:4 fatty acids.—Bolen, A. L., A. P. Naren, S. Yarlagadda, S. Beranova-Giorgianni, L. Chen, D. Norman, D. L. Baker, M. M. Rowland, M. D. Best, T. Sano, T. Tsukahara, K. Liliom, Y. Igarashi, and G. Tigyi. **The phospholipase A₁ activity of lysophospholipase A-I links platelet activation to LPA production during blood coagulation.** *J. Lipid Res.* 2011. 52: 958–970.

This work was supported by National Institutes of Health grant CA-092160 (G.T.), the Van Vleet Oncology Research Endowment (G.T.), the Gerwin Graduate Fellowship (A.L.B.), and the American Heart Association (A.L.B.). Its contents are solely the responsibility of the authors and do not necessarily represent the official views of the National Institutes of Health or other granting agencies.

Manuscript received 2 December 2010 and in revised form 24 February 2011.

Published, JLR Papers in Press, March 9, 2011
DOI 10.1194/jlr.M013326

Supplementary key words lysophospholipid • acyl protein thioesterase • autotaxin • lysophosphatidic acid

Lysophosphatidic acid (LPA) is a multifunctional phospholipid mediator and second messenger responsible for a wide variety of cellular responses (1–4). LPA elicits its actions through cell surface G protein-coupled receptors (GPCR) (1–4) and through the nuclear peroxisome proliferator activating receptor γ (PPAR γ) (5). LPA has been shown to play a role in many physiological functions and human diseases (1–4). The biochemical pathways involved in LPA production in biological fluids are not yet fully understood.

LPA can be produced by several intra- and extracellular biochemical pathways. Intracellularly, LPA is synthesized by a glycerophosphate acyl transferase-catalyzed reaction of glycerol-3-phosphate with acyl-CoA in the endoplasmic reticulum and mitochondria (6, 7). LPA has also been

Abbreviations: ACD, acidic citrate dextrose; APT1, acyl protein thioesterase 1; ATX, autotaxin; FP, fluorophosphonate; GPCR, G protein-coupled receptor; LCAT, lecithin-cholesterol acyltransferase; LPA, lysophosphatidic acid; LPC, lysophosphatidylcholine; LPL, lysophospholipid; LPS, lysophosphatidylserine; lyso-PAF, 1-oleyl-*sn*-glycero-3-phosphocholine; LYPLA-I, lysophospholipase A-I; MGLL, monoglyceride lipase; PC, phosphatidylcholine; PLA₁, phospholipase A₁; PRP, platelet-rich plasma; PS, phosphatidylserine; RH, rhodamine; sup, supernatant.

¹ Present address of T. Sano: Brain Science Institute, RIKEN, Saitama 351-0198, Japan.

² Present address of T. Tsukahara: Department of Integrative Physiology and Bio-System Control, Shinshu University School of Medicine, Matsumoto, Nagano 390-8621, Japan.

³ To whom correspondence should be addressed.

e-mail: gtigyi@uthsc.edu

[§] The online version of this article (available at <http://www.jlr.org>) contains supplementary data in the form of text.

shown to be generated in a spatially regulated fashion by the Ca^{2+} -independent phospholipase A_2 at the leading edge of migrating monocytes (8, 9). Third, acylglycerol kinase phosphorylates monoacylglycerol to form LPA (10). A fourth pathway in humans involves phosphatidylserine (PS)-specific phospholipase A_1 (PS- PLA_1) that generates lysophosphatidylserine (LPS), which in turn is converted to LPA by phospholipase D in mast cells (11, 12).

Extracellularly, LPA can be produced by a secretory phospholipase A_2 (PLA_2) (13), oxidative modification of low density lipoprotein (14), or by the action of phosphatidic acid-specific phospholipase A_1 (12, 15). However, the most important pathway is a multistep process linked to the activation of platelets (16–21). This mechanism involves release of unidentified PLA_1 and/or PLA_2 enzymes from activated platelets, thus generating a new pool of lysophospholipid (LPL) substrates, which in turn is cleaved by the lysophospholipase D autotaxin (ATX) (22, 23). As a result of this mechanism, plasma LPA concentration rises from a steady-state concentration of approximately 100 nM to serum concentrations up to 10 μM , with a significant increase in the content of polyunsaturated acyl species (19, 24, 25). The role of ATX in LPA production has been clearly demonstrated by the decreased plasma LPA level in ATX knockout mice (26, 27).

The rank order of the acyl species of LPA in normal human plasma is 18:2 > 18:1 > 18:0 > 16:0 > 20:4. In contrast, the rank order of the LPA acyl species in serum changes to 20:4 > 18:2 > 16:0 > 18:1 > 18:0 (19). The various acyl species of LPA also have differing ligand properties at target LPA GPCR (28). In addition to the differences in carbon chain length and degree of unsaturation, the PLA_3 and P2RY5 (PLA_6) receptors show a preference for the *sn*-2 over the *sn*-1 acyl regioisomer of LPA (29, 30). However, the *sn*-2 LPA regioisomer is relatively unstable. At neutral pH, acyl migration begins immediately to yield the more thermodynamically stable *sn*-1 regioisomer; an equilibrium ratio of 9:1 occurs between the two forms (31).

The linoleoyl (18:2) and arachidonoyl (20:4) species make up 84% of the LPA found in serum (19). The mechanism behind the enrichment and increase in polyunsaturated LPA species upon blood coagulation is still unknown. Because plasma phospholipids containing 18:2 and 20:4 fatty acids are almost exclusively esterified to the *sn*-2 glycerol carbon, we hypothesized that LPA in serum enriched in these fatty acyl species must be generated by the action of a PLA_1 enzyme (19). This hypothesis implies that the nascent *sn*-2 LPL generated by PLA_1 will either be rapidly cleaved by ATX and then undergo acyl migration or, alternatively, undergo acyl migration prior to headgroup cleavage. Distinguishing between the latter two possibilities is challenging due to the short half-life of the *sn*-2 LPLs that precludes the use of classical biochemical separation and analytical techniques.

In the present study, we sought to identify the putative PLA_1 enzymes released from activated platelets that are responsible for the generation of polyunsaturated LPL. Starting with the supernatants from thrombin-activated human platelets, we isolated lysophospholipase A1/acyl

protein thioesterase 1 (LYPLA-I/APT1) using a series of chromatographic steps and fluorophosphonate (FP)-biotin affinity labeling-based proteomics. LYPLA-I/APT1 transcripts were shown to be abundantly expressed in platelets and in megakaryocytes. LYPLA-I/APT1 was found to possess PLA_1 activity against plasma phospholipids, did not degrade LPA, and increased LPA production when added to plasma through the production of a pool of LPL, which is further cleaved by ATX.

MATERIALS AND METHODS

Fluorescently labeled 1-oleoyl-2-[12-[(7-nitro-2-1,3-benzoxadiazol-4-yl)amino]lauroyl]-*sn*-glycero-3-phosphoserine (NBD-PS 18:1-12:0), 1-oleoyl-2-[12-[(7-nitro-2-1,3-benzoxadiazol-4-yl)amino]lauroyl]-*sn*-glycero-3-phosphocholine (NBD-PC 18:1-12:0), dioleoyl phosphatidylserine (PS), linolenoyl phosphatidylcholine (PC), oleoyl LPA, LPC 17:0, and LPA 17:0 were purchased from Avanti Polar Lipids, Inc. (Alabaster, AL). 1-Oleoyl-*sn*-glycero-3-phosphocholine (lyso-PAF 18:1) was purchased from Bachem (Torrance, CA). Fluorophosphonate-rhodamine (FP-RH) and fluorophosphonate-biotin (FP-biotin) were a gift from Dr. Ben Cravatt (Scripps Institute, La Jolla, CA). Freshly expired apheresis platelets were provided by the Regional Medical Center (Memphis, TN), Methodist University Hospital (Memphis, TN), or purchased from Key Biologics, Inc. (Memphis, TN). PGE_1 and thrombin were obtained from Sigma-Aldrich (St. Louis, MO). Trizol and Superscript III OneStep RT-PCR were purchased from Invitrogen (Carlsbad, CA).

Isolation and activation of human platelets

The procedures detailed below were reviewed and approved by the Institutional Review Board of the University of Tennessee Health Science Center. Small-scale batches of platelet-rich plasma (PRP) were prepared by adding 3.6 ml acidic citrate dextrose (ACD, 0.8% citric acid, 2.2% sodium-citrate, 2.45% glucose) to 20 ml of cubital venous blood drawn from a volunteer donor and centrifuged at 180 g for 15 min. The top layer of PRP (~10 ml) was transferred to a new tube. For large-scale purifications, units of freshly expired apheresis platelets in ACD were obtained (approximately 60 ml per unit). Then 10 ml of the PRP from the small-scale purification or 10 ml of the apheresis platelets were diluted with 34 ml buffer A (138 mM NaCl, 3.3 mM NaH_2PO_4 , 2.9 mM KCl, 1 mM MgCl_2 , 20 mM HEPES, 1 mg/ml glucose, pH 7.5), and 1 μM PGE_1 was added. The diluted PRP was centrifuged at 1400 g at room temperature for 15 min. The supernatant was discarded, and the pellet containing the platelets was reconstituted in 2 ml buffer A, and 2 mM Ca^{2+} was added. The platelets were activated using 1 U thrombin per 1 ml sample at 37°C for 20 min, and the aggregate formed was centrifuged at 9,300 g for 5 min to yield supernatant 1 (Sup1). The Sup1 was then centrifuged again at 100,000 g for 45 min to remove platelet microvesicles. This preparation was designated as supernatant 2 (Sup2).

Measurement of phospholipase A_1 activity

PLA_1 activity was measured by determining the amount of lysophosphatidylcholine (LPC) or lysophosphatidylserine (LPS) generated after incubation of sample with phosphatidylcholine (PC) or phosphatidylserine (PS). NBD-PC or NBD-PS (45 ng to 2 μg) was incubated in 10 mM Tris (pH 7.5) or Sup2 (pH 7.5) at 37°C for 1 min to 1 h with or without an equal weight of BSA in water. For quantification, 900 ng, 90 ng, and 9 ng of the fluorescent substrates were incubated without enzyme for construction

of a standard curve by plotting fluorescence intensity as a function of substrate mass. Water-saturated butanol (BuOH) was added (30-120 μ l) to stop the reaction and extract the lipids. Samples (10 μ l) were spotted on Silica Gel 60 TLC plates. The plates were then developed with solvent A consisting of chloroform:methanol:ammonium hydroxide (V/V/V, 6:4:1) for NBD-PS, and solvent B consisting of chloroform:methanol:28% ammonium hydroxide:water (V/V/V/V, 50:40:8:2) for NBD-PC. The products were visualized using a Fotodyne imager (Hartland, WI) and quantified by the TotalLab100 software. The amount of the product generated was determined by interpolation from the standard curve. The Rf values for the various lipids were as follows: NBD-PC, 0.54; NBD-LPC, 0.38; NBD-FA, 0.77; NBD-PS, 0.45; NBD-LPS, 0.33; and NBD-FA, 0.67.

For unlabeled substrates, 10 μ g PC, PS, or LPA was digested at 37°C for 1 h in the presence of 10 μ g BSA. LPC 17:0 and LPA 17:0 (500-2000 ng in DMSO) internal standards were added prior to addition of 60 μ l BuOH. The samples were vortexed for 1 min, and the BuOH phase was isolated by centrifugation at 14000 *g* for 1 min and dried under argon. The lipid extract was reconstituted in 30 μ l methanol:acetonitrile:isopropanol:water (V/V/V/V, 1:1:1:1). LPC and LPA concentrations were determined by LC-MS/MS using an Applied Biosystems Sciex ABI 4000 QTRAP tandem mass spectrometer (Foster City, CA) equipped with a Turboionspray™ interface, a Shimadzu LC-10ADvp HPLC pump (Columbia, MD) with a Leap HTS PAL autosampler (Carrboro, NC). Samples (10 μ l) were injected onto a Tosoh TSK-ODS-100Z silica column (150 mm \times 2 mm; 5 μ m particle size) with a solvent consisting of methanol/water (V/V, 95:5) and 5 mM ammonium formate using an isocratic flow rate of 0.22 ml/min (32). The spectra were processed using Analyst software, version 1.5. The molecular species of LPC and LPA were analyzed by multiple reaction monitoring (MRM) in positive ion mode for LPC and negative ion mode for LPA. The Q3 (product ion) was set at *m/z* 184.0 for LPC and 153.0 for LPA (glycerophosphate moiety) (32). Q1 was set for the neutral molecular ion for all LPLs. Quantification was done by calculating the ratio of peak area to that of the appropriate LPC/LPA 17:0 internal standard and interpolated from the respective standard curve.

Partial purification of PLA₁

PLA₁ was partially purified using sequential chromatography on an AKTA FPLC system (GE Biosciences, Piscataway, NJ) by loading 330 mg (75 mg/ml) Sup2 to a Q Sepharose Fast Flow ion exchange chromatography column (GE Biosciences, 2 cm \times 10 cm). The column was eluted with a NaCl gradient (0-1 M) at a 1 ml/min flow rate over 20 min with buffer C (3.3 mM NaH₂PO₄, 2.9 mM KCl, 1 mM MgCl₂·6H₂O, 20 mM HEPES, pH 7.5). The PLA₁ active fractions were combined, and 5 ml (~30 mg) was loaded onto a Butyl-Sepharose hydrophobic interaction chromatography column (GE Biosciences, 0.7 cm \times 2.5 cm, 20 mg/ml medium). The column was eluted using a gradient from 1.7 M to 0 M (NH₄)₂SO₄ over 20 min in 0.05 M Na₂HPO₄ buffer (pH 7.6). The active fractions were combined, and 5 ml (~2.5 mg) was loaded onto a HiTrap Blue affinity chromatography column (GE Biosciences, 0.7 cm \times 2.5 cm). The column was eluted by increasing (NH₄)₂SO₄ from 0 M to 1.7 M over 20 min in 0.05 M Na₂HPO₄ buffer (pH 7.6). An amount of 3 ml fractions were collected at each step. An amount of 100 μ l of each fraction was used for PLA₁ activity measurement using 1 μ g NBD-PS substrate at 37°C for 2 h. An amount of 120 μ l water-saturated BuOH was added to stop the reaction and extract the lipids. The samples were vortexed and centrifuged for 1 min at 14,000 *g*. Then 10 μ l of the BuOH phase was spotted to a Silica Gel 60 TLC plate. The plate was developed with solvent A, and the products were visualized. The fractions with PLA₁ activity from each chromatographic step were combined, activity was determined as described, and pro-

tein concentration was determined by BCA protein assay (Pierce, Rockford, IL) following the manufacturer's protocol.

FP-RH labeling

An amount of 50 μ g protein of the PLA₁ active Butyl-Sepharose pooled fractions (~100 μ l) and 0.9 μ g NBD-PS substrate was incubated at 37°C for 3 h with 0.03, 0.1, 0.3, 1, 3, 10, and 30 μ M FP-RH. Then 60 μ l water-saturated BuOH was used to stop the reaction and extract the lipid products. After mixing, the samples were centrifuged for 1 min at 14,000 *g*. Then 10 μ l of the BuOH phase was spotted to a Silica Gel 60 TLC plate and developed with solvent A. The products were visualized using a Photodyne imager and quantified using standards run alongside the samples on the same TLC plate.

FP-biotin labeling and purification

The activity-based proteomic probe, FP-biotin, was used to label all serine hydrolases in the PLA₁-active HiTrap Blue fractions. An active pool of HiTrap Blue chromatography fractions was concentrated using an Amicon concentrator (Millipore, Billerica, MA) with a 5 kDa molecular weight cutoff. An amount of 1 mg protein (1 mg/ml) was incubated for 2 h with a final concentration of 5 μ M FP-biotin. Streptavidin beads (Pierce, Rockford, IL) were prewashed three-times with binding buffer (0.1 M sodium phosphate, 0.15 M NaCl, pH 7.0) followed by centrifugation (3000 *g* for 1 min), and the supernatant was discarded. The protein complex was added to 50 μ l resin and incubated with mixing for 1 h at room temperature. Streptavidin-bound FP-biotinylated proteins were washed with binding buffer in the presence of 4 M urea, 0.1% SDS (W/V), and 0.2% TritonX-100 (V/V) (pH 7.2), and then centrifuged for 1 min at 3000 *g*. The supernatant was removed, and the wash procedure was repeated four times. The beads were reconstituted in 1 ml 50 mM TRIS-HCl (pH 7.2), centrifuged for 4 min at 10,000 *g*, and the supernatant was decanted. An amount of 200 μ l 50 mM TRIS-HCl (pH 7.2) was added to reconstitute the final pellet.

Proteomic analysis of FP-biotin-labeled products in partially purified platelet supernatants

The bead-bound FP-biotin-labeled proteins were first reduced with 5 mM dithiothreitol for 30 min at room temperature and alkylated with 10 mM iodoacetamide at room temperature in the dark for 30 min. The sample was centrifuged for 4 min at 10,000 *g*, and then 100 μ l of supernatant was removed. A total of 300 μ l 50 mM TRIS (pH 7.2) buffer and 1.5 μ l of 0.5 μ g/ μ l trypsin (sequencing grade, Sigma-Aldrich, St. Louis, MO) was added and incubated at 37°C for 12 h. The sample was centrifuged for 4 min at 10,000 *g*, and the supernatant containing the peptide digest was transferred to a new tube; formic acid was added to a final concentration of 5% (V/V). The volume of the peptide sample was reduced to 40 μ l in a vacuum centrifuge. The peptides were desalted with a Zip Tip C18 microcolumn (Millipore, Billerica, MA) using the procedure recommended by the manufacturer. Peptides were eluted using 4 μ l of 50% acetonitrile/0.1% trifluoroacetic acid (V/V). Four microliters of water/acetic acid (0.5%) were added to the sample. LC-MS/MS experiments were performed on an LTQ linear ion trap mass spectrometer (Thermo Scientific, Waltham, MA) coupled to a nanoflow LC system (Dionex, Sunnyvale, CA). The peptide sample was injected onto a fused-silica capillary column/spray needle (15 cm length, 75 μ m ID; New Objective, Woburn, MA) packed in-house with C18 stationary phase (Michrom Bioresources, Auburn, CA). The peptides were separated with a 90 min gradient from 0% to 90% of mobile phase B. The composition of mobile phase B was 90% MeOH/10% water/0.05% HCOOH; the composition of mobile

phase A was 2% MeOH/98% water/0.05% HCOOH. Mass spectrometric data acquisition was performed in the data-dependent mode; one cycle encompassed a full-range MS scan followed by seven MS/MS scans on the most abundant ions from the MS scan. The LC-MS/MS data were used to search the SwissProt protein sequence database (subset of human proteins), using the program Bioworks/Sequest (Thermo Scientific).

RNA purification and RT-PCR

A total of 100 ml of venous blood was drawn into 20 ml ACD, 1 μ M PGE₁. The blood was centrifuged at 180 g, and the PRP was filtered through a PL6T leukocyte reduction filter (Pall, Inc., Port Washington, NY). Buffer A (68 ml) and 12 ml ACD was added to the sample and centrifuged at 1,400 g. The supernatant was removed, the platelet pellet was resuspended in 1 ml Trizol (Invitrogen), and RNA was extracted following the manufacturer's protocol. Two gene- and species-specific primers for each candidate protein were designed. Each primer was designed to produce a product between 250 and 350 basepairs long and span an intron of more than 1,000 base pairs so that DNA contamination would easily be identifiable by the size of the product. The following primers were used: LYPLA-I/APTI 1: 5'-GCAGAAGCCTT TGCAGGTAT -3', forward 5'-ATTGCCATTCTTCACTTCTTGAT-3', reverse; LYPLA-I/APTI 2: 5'-ACTCAGTTGCTGGCTTCCAC-3', forward 5'-TGCTTGACATCCATCATTTCC-3', reverse; MGLL 1: 5'-GCTGGACCTGCTGGTGT-3', forward 5'-TGTTGCAGATTCAGGATTGG-3', reverse; MGLL 2: 5'-AAGGGGCTACCTGCTCAT-3', forward 5'-TGGCTGTCTTTGAGAGACC-3', reverse; PLA1A 1: 5'-CCAATGATGTGGATTGAGGA-3', forward 5'-GAA-GCCATCCACACACACAC-3', reverse; PLA1A 2: 5'-GCTGTGGGAGCTAGTAGAAC-3', forward 5'-CCAATGATGTGGATTGAGGA-3', reverse; LCAT 1: 5'-3', forward 5'-3', reverse; LCAT 2: 5'-GCTCCTCAAT GTGCTCTTCC-3', forward 5'-CGGTAGCATCCAGTTCAC-3', reverse. RT-PCR was done using the Superscript III kit (Invitrogen). Thirty cycles were performed using 400 ng RNA template. The PCR products were separated on 2% agarose gels and visualized with ethidium bromide staining.

MGLL activity assay

Human recombinant monoglyceride lipase (MGLL) was purchased from Abnova Corporation. An amount of 0.5 μ g enzyme was incubated with NBD-PS (0.9 μ g) for 3 h at 37°C in 20 μ l 10 mM TRIS (pH 7.5). Then 30 μ l water-saturated BuOH was added to extract the lipids, and 10 μ l of the extract was spotted on a TLC plate. The plates were then developed with solvent A consisting of chloroform:methanol:ammonium hydroxide (V/V/V, 6:4:1). The products were visualized using a Fotodyne imager (Hartland, WI) and quantified by the TotalLab100 software. The amount of the product generated was determined by interpolation from the standard curve.

Recombinant MGLL was purchased from Abnova Corporation (Jhongli, Taiwan) and tested for activity using an assay kit from Cayman Chemicals (Ann Arbor, MI) that utilizes the hydrolysis of the thioester bond of arachidonoyl-1-thio-glycerol to produce a free thiol that reacts with 5,5'-dithiobis-(2-nitrobenzoic acid) (DTNB). Recombinant MGLL (0.3 μ g or 0.5 μ g) or 100 μ l PLA₁-active Blue-Sepharose fraction was added in 150 μ l total volume with assay buffer (10 mM TRIS-HCl, 1 mM EDTA, pH 7.2), to a 2.7 mM ethanolic solution of arachidonoyl-1-thio-glycerol and incubated at room temperature for 5 min. The absorbance was read at 415 nm using a BioTek microplate reader.

Construction of recombinant LYPLA-I/APTI expression plasmid

Human full-length LYPLA-I/APTI (Accession #AF081281) was PCR-amplified. The PCR products were cleaned using the

Qiagen PCR purification kit and eluted in 20 μ l DNA grade water. The DNA was used for ligation-independent cloning (LIC) using the Ek/LIC cloning kit from Novagen (EMD, Gibbstown, NJ). Primers used for LIC cloning were: LYPLA-I/APTI-full-length-LIC forward: GACGACGACAAGATGTGCGGCAA TAA-CATGTCAACC and LYPLA-I/APTI-full-length-LIC reverse: GAGGAGAAG CCCGGTTCAATCAATTGGAGGTAGGAG. PCR-purified DNA (14.6 μ l) was taken into a sterile centrifuge tube, and 2 μ l each of 10 \times concentrated T4 DNA polymerase buffer and 25 mM dATP were added. One hundred millimolars dithiothreitol (1 μ l) and 0.4 μ l of T4 DNA polymerase were added to start the reaction with gentle stirring at 22°C for 30 min. The reaction was stopped by incubation at 75°C for 20 min. This T4 DNA polymerase-treated insert can be annealed into any Ek/LIC vectors, including the pET-41 vector used here. For the ligation reaction, 1 μ l Ek/LIC vector (pET-41) and 2 μ l of T4 DNA polymerase-treated insert were used and incubated at 22°C for 5 min. Then 1 μ l of 25 mM EDTA was added for 5 min at 22°C. The ligated product was transformed into Novablue cells (EMD biosciences, Gibbstown, NJ). Three transformants were picked, and plasmid DNA was isolated and sequenced. The sequences were confirmed to be those of LYPLA-I/APTI.

Recombinant LYPLA-I/APTI purification

GST-LYPLA-I/APTI was purified from transformed BL21-DE3 *E. coli* bacteria. Protein expression was induced using 200 μ M isopropyl β -D thiogalactopyranoside. Bacteria were pelleted by centrifugation and resuspended in lysis buffer (50 mM TRIS base, 1 mM EDTA, and 10% sucrose containing the protease inhibitors; aprotinin 1 μ g/ml, leupeptin 1 μ g/ml, pepstatin 1 μ g/ml, and PMSF 500 μ M). Lysozyme (1 mg/ml) was added to the resuspended bacteria and allowed to mix at 4°C for 30 min. NP40 was added to the suspension (0.2% final concentration) and allowed to mix at 4°C for 30 min. The suspension was cleared by centrifugation at 14,000 g for 30 min at 4°C. Glutathione beads (ThermoFisher Scientific; 2 ml of 50% slurry) were added to the cleared supernatant and allowed to mix for 2 h at 4°C. Glutathione beads were retrieved by centrifugation and washed with 0.2% Triton-X-100 (V/V) in PBS three times, followed by a wash with PBS plus protease inhibitors. A 20 μ l sample of the protein bound to the glutathione beads was eluted using Laemmli sample buffer and run on a 4-15% gel to visualize the quantity and purity of the isolated protein. Protein was eluted from the beads using 20 mM reduced glutathione (pH 7.8) and dialyzed against an appropriate buffer and protein and stored in small aliquots at -80°C.

The GST tag was removed by thrombin cleavage using 1 mg of GST-LYPLA-I/APTI mixed with 2.5 units of biotinylated thrombin (Novagen, Darmstadt, Germany) in 20 mM TRIS-HCl (pH 8.4), 150 mM NaCl, 2.5 mM CaCl₂ buffer at 20°C for 16 h. After cleavage, the biotinylated thrombin was removed using streptavidin-agarose (Novagen) using a ratio of 16:1 settled resin per unit of enzyme.

Recombinant protein was tested for PLA₁ activity by incubating 0.5 μ g of LYPLA-I/APTI or 0.05 μ g GST-LYPLA-I/APTI with 0.9 μ g BSA and 0.9 μ g NBD-PS in 20 μ l of 10 mM TRIS-HCl (pH 7.6) for 15 min at 37°C. Water-saturated BuOH (30 μ l) was added to stop the reaction and extract the lipids after centrifugation. Samples (10 μ l) of the BuOH phase were spotted on Silica Gel 60 TLC plates, which were developed with solvent A. The products were visualized using a Fotodyne imager.

Monitoring LPC and LPA production in plasma

Blood (5 ml) was drawn into a heparinized or nontreated Vacutainer tubes. Blood was centrifuged at 14,000 g for 1 min, and the PRP was transferred to a new tube. The PRP from the tube

with no additive was allowed to clot to generate serum. An amount of 10 μg recombinant LYPLA-I/APT1 enzyme was added to 1 ml activated plasma and incubated at 37°C for 24 h alongside 1 ml activated plasma without addition of the enzyme. The internal standards 17:0 LPA and 17:0 LPC (20 ng each) were added to 200 μl of the fresh PRP or to 200 μl of the serum samples after 24 h incubation. A total of 200 μl of citrate phosphate buffer (30 mM citric acid and 40 mM Na_2HPO_4 , pH 4.0), 400 μl methanol, and 200 μl chloroform were added to the samples, and then centrifuged at 14,000 g for 1 min. The chloroform layer was transferred to a new tube, dried under argon gas, and reconstituted in 30 μl methanol:acetonitrile:isopropanol:water (V/V/V/V, 1:1:1:1). LPA 18:2 and LPA 20:4 were quantified by LC-MS/MS as described above.

Synthesis of sn-2 lyso-PAF 18:1

Synthesis and characterization of sn-2 lyso-PAF 18:1 is described in the online supplementary data.

Determination of regioisomeric selectivity of ATX against two lyso-PAF substrates

Serial dilutions of either sn-1 or sn-2 lyso-PAF 18:1 (2 mM to 31.25 μM in 20 μl assay buffer, 50 mM TRIS, pH7.4, 5 mM CaCl_2 , 1 mg/ml BSA) were added to the wells in a 96-well, half-area plate. A total of 20 μl of either 10 nM ATX (final concentration) or assay buffer was added to the wells, along with 20 μl Amplex Red cocktail [10 μM Amplex Red, 0.1 unit/ml choline oxidase (CO), and 1 unit/ml HRP, final concentration] (Amplex Red, Invitrogen, Carlsbad CA; CO, MP Biomedical, Solon OH; HRP, ThermoFisher Scientific, Waltham, MA). The plate was incubated at 37°C for 6 h and was read at excitation/emission wavelengths of 530/590 nm every 2 min with a BioTek Synergy 2 plate reader (Winooski, VT). A linear segment of time versus concentration of product was plotted for each substrate concentration to determine initial reaction velocity. To calculate product concentration, a linear segment of absorbance values of serial dilutions of resorufin (2,000-0.0004768 μM) was used to establish a calibration curve of resorufin fluorescence. Resorufin and product concentration are directly proportional in the Amplex Red assay; thus, experimental absorbance values were interpolated on the calibration curve to determine product concentration. Substrate concentration versus initial velocity was then plotted using GraphPad Prism[®] version 5.0a for Mac OS X, and a rectangular hyperbolic curve fit was used to define kinetic parameters.

RESULTS

Phospholipases released from activated platelets generate lysophospholipids, but LPA production requires ATX from plasma

Platelet activation triggers an upsurge in production of LPA molecular species, predominantly with 18:2 and 20:4 fatty acids (16–21, 24). Using biosynthetic labeling of platelet phospholipids, it has been shown that only trace amounts of ³²P-LPA were found in the supernatant of activated platelets (19). To extend this observation concerning the lack of LPA production by platelets, we tested the hypothesis that platelets secrete phospholipase(s) that de novo generate a pool of LPL, which in turn serves as substrates for ATX constitutively present in plasma (33–35). The first question we raised in pursuing this hypothesis was whether platelet activation by thrombin leads to the release of PLA₁ detectable in the supernatant. To deter-

mine this, PC18:2 (Fig. 1A), PS18:1 (Fig. 1B), NBD-PC (Fig. 1C), and NBD-PS (Fig. 1D) were incubated with Sup2 in the presence or absence of ATX. We found significant LPC generation in Sup2, regardless of whether we used PC 18:2 or NBD-PC as substrate. However, very little LPA was produced. Using the fluorescent NBD-PC substrate, LPA production was below the level of detection of our assay; however, using mass spectrometry, we detected a 0.028 ± 0.06 ng/ μg /h rate of LPA production. When PS 18:1 was used for substrate, we observed the production of LPS 18:1 and a higher rate of LPA production amounting to 4.2 ± 0.8 ng/ μg /h. However, using NBD-PS, we still were unable to detect LPA production. In contrast, when recombinant human ATX was added, a 9.5-fold increase in the amount of LPA generated from LPC and a 2-fold increase in the amount of LPA generated from LPS, with a concomitant decrease in the LPC or LPS, was observed. When NBD-PC or NBD-PS analogs were used, essentially the same findings were noted, validating the applicability of these fluorescent analogs for monitoring LPL production. The finding of high rates of LPC and LPS production in the Sup2 suggests that phospholipases are secreted from platelets, but lysophospholipase D is not present in sufficient quantity to provide for substantial LPA production. The results with NBD phospholipids indicate that substantial amounts of PLA₁ activity are present in Sup2, because the

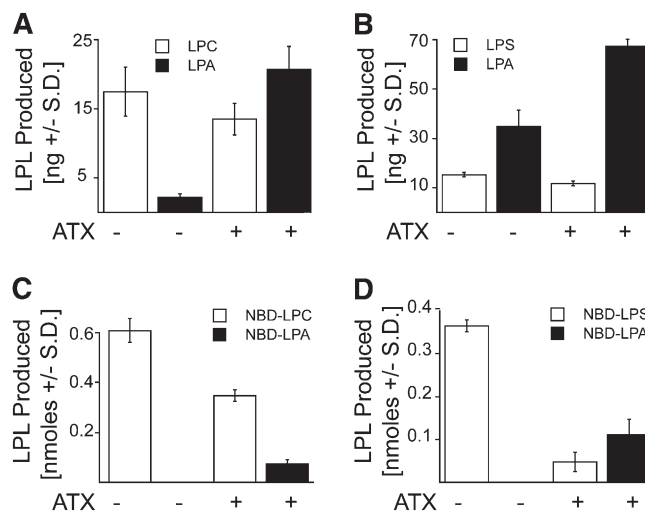


Fig. 1. ATX is required for LPA production in activated platelet supernatant. Supernatant from thrombin-activated human platelets was incubated in the absence or presence of recombinant human ATX with 10 μg PC 18:2 (A), 10 μg PS 18:1 (B), 1 μg NBD-PC 18:1/12:0 (C), or 1 μg NBD-PS 18:1/12:0 (D) supplemented with 250 μM BSA and 135 mM NaCl in the presence or absence of 200 nM ATX at 37°C for 1 h. Generation of the corresponding LPC and LPA species was quantified using LC/MS (A and B) or TLC (C and D). In the absence of added ATX, very little LPA was produced. In sharp contrast, LPC was abundantly generated by a PLA activity. Addition of ATX lead to a 9.5-fold increase in the amount of LPA generated from LPC and a 2-fold increase in the amount of LPA generated from LPS, with a concomitant decrease in the LPC or LPS. When the unnatural NBD-PC/PS analogs were used, essentially the same findings were noted, validating the usability of these fluorescent analogs for monitoring LPA production. Bars are the mean of three independent determinations \pm SD.

predominant products formed were NBD-LPC and NBD-LPS with the fluorescent label in the *sn*-2 position. We hypothesized that phospholipase(s) A₁ are secreted upon activation of platelets, and we next attempted to purify these enzymes.

Partial purification of PLA₁ from supernatants of activated human platelets

To further substantiate the hypothesis that a novel PLA₁ is secreted from platelets, we partially purified this enzyme from Sup2. Sup2 from human platelets was prepared and applied to Q Sepharose Fast Flow ion exchange chromatography using an AKTA FPLC system. Fractions (3 ml) were collected, and each fraction was assayed for PLA₁ activity using NBD-PS as a substrate. Most PLA₁ activity with low PLA₂ activity contamination was found in the last portion of the flow-through fractions, and no PLA₁ activity was detected in the bound fractions. The active fractions were combined and concentrated using a 5 kDa Amicon concentrator to exchange the buffer and loaded onto a Butyl-Sepharose column. The resulting active fractions were then loaded onto a HiTrap Blue affinity chromatography column to eliminate albumin from the sample, and the PLA₁ was recovered from the flow through and concentrated as above. The specific PLA₁ activity present in the various pooled fractions is shown in **Table 1**. The three chromatographic steps resulted in a 1,500-fold purification of PLA₁ activity.

Activity-based purification of platelet PLA₁

Even though the multistep chromatographic purification yielded a 1500-fold enrichment of PLA₁ activity, the sample contained multiple protein bands when examined using SDS-PAGE. Further chromatographic purification led to loss of activity, necessitating a change in the purification strategy. Most phospholipases contain a serine in the catalytic site that selectively reacts with fluorophosphate (36). Most serine hydrolases are potently inhibited by FP or its derivatives. However, FPs do not inhibit cysteine, aspartyl, or metalloproteases (37). Rhodamine- and biotin-labeled FP probes are rapid, selective, and highly sensitive affinity labels for serine hydrolases. In these probes, the fluorescent reactive group or the biotin tag is coupled through a long alkyl chain and two amide bonds (37).

We first determined if the PLA₁ activity present in platelets reacted with a FP probe. A Butyl-Sepharose fraction was incubated with incremental amounts of FP-RH and NBD-PS substrate. An increase in concentrations of FP-RH produced a decrease in NBD-LPS production, presumably due to competition between FP-RH and NBD-PS for the catalytic site of PLA₁ (**Fig. 2A**). This experiment provided evidence that PLA₁ was a serine hydrolase and reacted with

FP probes. FP-RH optimally inactivated PLA₁ at 5 μM and 2 h of incubation (data not shown).

Identification of serine hydrolases secreted from thrombin-activated human platelets

Since we determined that PLA₁ reacted with the FP probes, we then labeled the partially purified PLA₁ obtained after the HiTrap Blue chromatography step with FP-biotin. The FP probe allowed us to selectively label all serine hydrolases present in our sample, and the biotin allowed us to isolate the labeled proteins using streptavidin beads. We analyzed samples from three different purifications. MS/MS data were obtained for the tryptic peptides present in the digest. The MS/MS data, which are diagnostic of the peptide sequences, were used to identify the proteins of interest through protein database searches. Based on LC-MS/MS data, four relevant candidate proteins were identified: lecithin-cholesterol acyltransferase (LCAT), phosphatidylserine-specific phospholipase A₁ (PS-PLA₁), MGLL, and LYPLA-I, also known as APT1 (**Table 2**).

Because we used PRP as a starting material, plasma protein contamination in our sample was a possibility; hence, it was important to determine whether the proteins identified in the sample were expressed in platelets. To this end, mRNA was isolated from human platelets, and RT-PCR for LYPLA-I/APT1, MGLL, PLA1A, and LCAT was performed using two different gene-specific primer pairs (denoted 1 and 2, **Fig. 2B**). The eight primer sets were validated to amplify the appropriate transcripts derived from selected tissues. Only two of the four lipases identified by LC-MS/MS, namely LYPLA-I/APT1 and MGLL, yielded PCR products of the expected size, indicating the expression of these enzymes in human platelets.

We hypothesized that either MGLL or LYPLA-I/APT1 or both might play a role in LPA production during blood coagulation. To determine whether any of these proteins is involved in LPA production, we needed to first establish whether either enzyme possessed PLA₁ enzymatic activity. Human recombinant MGLL was tested for PLA₁ activity (**Fig. 2C**). No cleavage of NBD-PS or generation of NBD-LPS product was detected, suggesting that it does not function as a PLA₁. Using as much as 0.5 μg recombinant MGLL in a MGL activity assay (**Fig. 2D**), we verified that the enzyme was active even though it lacked PLA₁ activity. Furthermore, using the Blue-Agarose fraction rich in PLA₁ activity, we were unable to detect MGLL activity using the same assay. These results suggested that MGLL does not have PLA₁ activity and, therefore, is unlikely to contribute to the production of LPA during blood coagulation.

TABLE 1. Summary of chromatographic steps

Step	μg Protein/μl	Specific Activity (units ^a /μg)	Purification (fold)
Platelet Supernatant (Sup2)	75.3 ± 6.2	0.10 ± 0.03	1
Q Sepharose	16.2 ± 1.7	1.6 ± 0.4	16
Butyl Sepharose	0.08 ± 0.02	89.2 ± 4.4	872
HiTrap Blue	0.03 ± 0.01	159.5 ± 27.6	1560

^aUnits defined in nanomoles of LPS formed per h at 37°C.

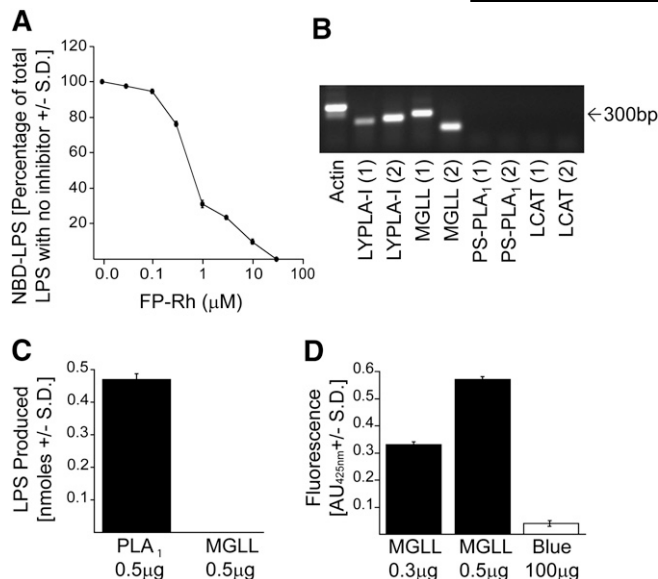


Fig. 2. FP-RH binds to PLA₁, inhibiting activity and NBD-LPS production. Incremental amounts of FP-RH were incubated with NBD-PS and a phospholipase A1 active Butyl-Sepharose fraction (A). The production of NBD-LPS decreased with increasing amounts of FP-RH. Expression of serine hydrolase transcripts in human platelets (B). RT-PCR for LYPLA-I/APTI, MGLL, PS-PLA₁, and LCAT was performed using two different gene-specific primer pairs (denoted 1 and 2) using mRNA isolated from human purified platelets. Only LYPLA-I/APTI and MGLL amplification yielded PCR products of the expected size, indicating the expression of these enzymes in human platelets. These results were confirmed with platelets from five other donors of both sexes. MGLL does not possess PLA activity (C and D). When incubated with NBD-PS, no LPS formed, which indicated MGLL does not possess PLA activity (C). Human recombinant MGLL was shown to have MGL activity to prove functionality (D). Bars are the mean of three independent determinations ± SD.

We next tested whether LYPLA-I/APTI functioned as a PLA₁. Human recombinant GST-LYPLA-I/APTI was expressed and purified from transformed *E. coli*. Coomassie Blue-stained SDS-PAGE showed that the purified GST-tagged LYPLA-I/APTI and the LYPLA-I/APTI with the GST tag removed yielded a single protein band with the expected 25 kDa size (Fig. 3A). PLA₁ activity assays using

1 μg NBD-PC in 20 μl 10 mM TRIS (pH 7.9) at 37°C for 10 min performed on GST-tagged LYPLA-I/APTI and thrombin-cleaved LYPLA-I/APTI showed no detectable PLA₁ activity with GST-tagged enzyme (Fig. 3B). In contrast, the LYPLA-I/APTI with the tag removed showed activity when incubated with NBD-PC, indicating that the GST tag inhibits activity of the enzyme and that LYPLA-I/APTI possesses phospholipase A₁ activity.

Recombinant human LYPLA-I/APTI acts primarily as a phospholipase A₁ and does not break down LPA

LYPLA-I/APTI has two known functions to date. As an acyl-protein thioesterase, it has been shown to deacylate G proteins and other thioacylated protein substrates (38). As a lysophospholipase, it cleaves the remaining fatty acid from either carbon of the glycerol backbone of lysophosphatidylcholine or lysophosphatidylserine. Because this protein has lysophospholipase activity, it was challenging to separate the PLA₁ activity from the lysophospholipase activity, as the product of the PLA₁ activity is also the substrate of the lysophospholipase activity. Using unlabeled substrate to measure PLA₁ activity of the recombinant enzyme was not feasible, as we were unable to distinguish how much of the product was being cleaved by the lysophospholipase activity, precluding the determination of the specific PLA₁ catalytic activity. To establish a timeline for the dual activities of the same enzyme, we used NBD-PC, which allowed us to independently monitor the generation of NBD-LPC (product of PLA₁ cleavage) and NBD-FA (product of LYPLA-I/APTI cleavage) products for both enzymatic activities and at least initially monitor reaction preference. NBD-PC, NBD-LPC, and NBD-FA were quantified as percentage of total substrate and product (Fig. 4A). Eleven percent of added NBD-PC was converted to NBD-LPC within 1 min, indicating the robust PLA₁ activity of the enzyme. In contrast, NBD-FA production reached a comparable amount only after 5 min of incubation, further signifying that the initial and preferred product of LYPLA-I/APTI was NBD-LPC. NBD-LPC reached a maximum steady-state level of 25% after 5 min, whereas NBD-FA generation continued steadily with the availability of NBD-LPC substrate for the LYPLA-I/APTI

TABLE 2. LC-MS/MS candidate protein peptide sequences

Protein Name	Entry Name	Accession Code	Theoretical Molecular Weight (kDa)	Peptide Sequence	Occurrence of Peptide in Samples
Lecithin-cholesterol acyltransferase	LCAT_HUMAN	P04180	67	DLLAGLPAPGVEVYC*LYGVGLPTPR	3
				TYSVEYLDSSK	2
				SSGLVSNAPGVQIR	4
				LDKPDVNVWM#C*YR	3
				ITTTSPWMFPSR	3
				TYNDHGFYTDVPGVLYEDGDDTVATR	2
Lysophospholipase A-I	LYPA1_HUMAN	O75608	25	LAGVTALSC*WLPLR	3
				ASFPQGPPIGGANR	5
				TYEGMMHSSC*QQEMMDVK	5
				TLVNPANVTFK	6
				FC*TALLPVNDR	1
Phosphatidylserine-specific PLA ₁	PLA1A_HUMAN	Q53H76	55	C*ADFQSANLFEGTDLK	1
				LTVPFLLQGSADR	1
Monoglyceride lipase	MGLL_HUMAN	Q99685	59		

In peptide sequences, C* indicates carbamidomethylated cysteine, and M# indicates oxidized methionine.

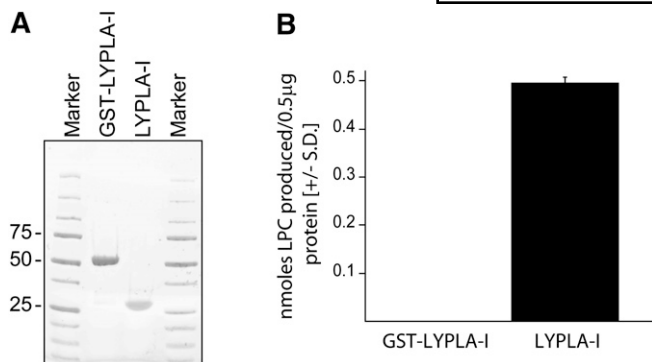


Fig. 3. Human recombinant LYPLA-I/APTI with and without a GST tag were purified for analysis (A). Coomassie Blue-stained SDS-PAGE gels show the protein profiles of the GST-tagged LYPLA-I/APTI protein and the thrombin-cleaved LYPLA-I/APTI protein (5 µg each). Human recombinant LYPLA-I/APTI must be unlabeled for functionality (B). PLA activity assay was performed on both GST-tagged LYPLA-I/APTI and thrombin-cleaved untagged LYPLA-I/APTI (0.5 µg each). No activity was found when the GST tag was present. The thrombin-cleaved version of LYPLA-I/APTI had abundant PLA₁ activity when incubated with NBD-PC in the presence of BSA. Bars are the mean of three independent determinations ± SD.

activity of the enzyme. NBD-FA product could also be generated by PLA₂ cleavage of NBD-PC; however, this product was not seen initially, making such catalytic activity unlikely. Along with the generation of NBD-LPC and NBD-FA, there was a continuous decrease in the NBD-PC substrate. This time course is consistent with the hypothesis that human recombinant LYPLA-I/APTI acts preferentially as PLA₁ and only secondarily as LYPLA-I/APTI.

The hypothesis that LYPLA-I/APTI would supply LPL to ATX and thereby contribute to LPA production could only be sustained if LYPLA-I/APTI did not cleave LPA and degrade it. To test this hypothesis, recombinant LYPLA-I/APTI was incubated with LPA 18:1 for up to 1 h, and the amount of LPA degraded was quantified by LC-MS/MS (Fig. 4B). The amount of LPA did not decrease during the 1 h incubation, indicating that LPA is not a substrate for LYPLA-I/APTI. Therefore, LYPLA-I/APTI does not contribute to the degradation of LPA.

LYPLA-I/APTI contributes to the production of LPA during blood coagulation

The predominance of 18:2 and 20:4 LPA species in serum indicates that PLA₁ cleavage must be involved in this biochemical pathway as these fatty acids are overwhelmingly esterified to the *sn*-2 carbon of phospholipids. ATX has low, but constitutive activity for *sn*-1 LPC present in plasma, indicated by the low concentration of LPA and the rather slow increase in LPA in heparinized plasma *ex vivo* (Fig. 5A, B) (19). Therefore, ATX alone cannot account for the upsurge in LPA production subsequent to activation of blood clotting. We hypothesized that LYPLA-I/APTI release from activated platelets is, at least in part, responsible for the increase in LPA production by supplying a newly formed pool of LPL to ATX upon the activation of platelets. To examine this, heparinized plasma and

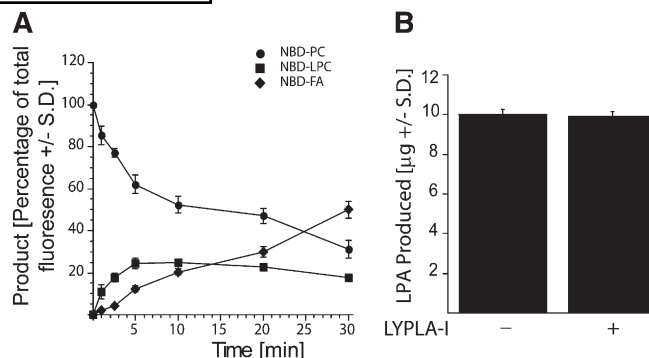


Fig. 4. Human recombinant LYPLA-I/APTI acts first as PLA₁, and then has lysophospholipase activity when incubated with NBD-PC (A). Purified human recombinant LYPLA-I/APTI was incubated with NBD-PC and BSA for 0, 1, 2.5, 5, 10, 20, and 30 min. NBD-LPC was generated immediately, indicating PLA₁ activity of the enzyme. After the initial generation of NBD-LPC, NBD-FA was generated, indicating a lysophospholipase activity of the enzyme with a simultaneous decrease in the starting substrate. Human recombinant LYPLA-I/APTI did not cleave LPA, and therefore, did not contribute to the breakdown of LPA (B). LYPLA-I/APTI was incubated with LPA 18:1 in the presence of BSA for 1 h. The amount of LPA did not decrease during incubation, indicating that LPA is not a substrate for LYPLA-I/APTI. Bars are the mean of three independent determinations ± SD.

human activated plasma generated by physiological means in venous blood were incubated with or without exogenously added human recombinant LYPLA-I/APTI for 24 h, and the production of polyunsaturated LPA species was quantified using LC-MS/MS. On addition of LYPLA-I/APTI, LPA 18:2 (Fig. 5A) and LPA 20:4 (Fig. 5B) began increasing in a time-dependent manner in physiologically activated plasma. By the end of the 24 h incubation, addition of LYPLA-I/APTI to the activated plasma significantly increased the amount of LPA 18:2 and 20:4. The generation of these LPA species in activated plasma without the addition of LYPLA-I/APTI also increased but to a much lower extent compared with the LYPLA-I/APTI spiked samples. Note that these samples contained endogenous

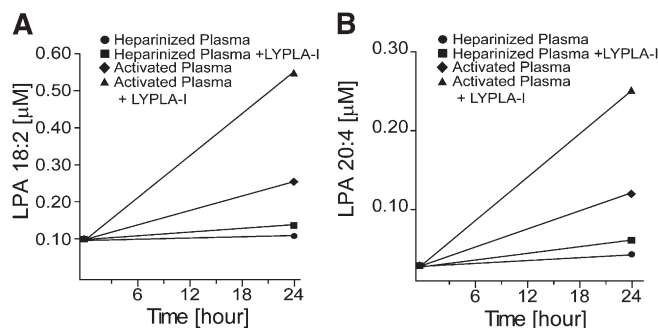


Fig. 5. Human recombinant LYPLA-I/APTI increases the amount of LPA 18:2 and LPA 20:4 in a time-dependent manner. Physiologically activated plasma and plasma with heparin additive were incubated with or without human recombinant LYPLA-I/APTI for 24 h. LPA 18:2 and LPA 20:4 in activated plasma began increasing after 3 h and increased greatly at 24 h. In contrast, in heparinized plasma LPA 18:2 and LPA 20:4 showed no increase, except in the sample with LYPLA-I/APTI at 24 h.

LYPLA-I, which also contributed to the production of LPC. There was no significant increase in either LPA species when platelet activation was prevented by heparin and removal of plasma from the blood cells within 5 min of blood collection. However, there was a small increase at 24 h with the addition of LYPLA-I/APT1 to heparinized plasma, suggesting the enzyme could utilize physiological substrates. We also determined that heparin (18.75 U/ml) used for anticoagulation of blood inhibited 90% of the activity of ATX, although it did not inhibit the phospholipase A₁ activity of LYPLA-I/APT1 (data not shown).

To extend these observations, we tested the effect of exogenous LYPLA-I/APT1 addition on LPA 18:2 and LPA 20:4 production in a small sample of human donors from both sexes. Activated plasma was incubated with or without 10 µg/ml human recombinant LYPLA-I/APT1 for 24 h, and the amount of LPC 18:2, LPC 20:4, LPA 18:2, and LPA 20:4 was quantified using LC-MS/MS. LPC 18:2 (Fig. 6C) increased significantly by 1.5-fold with the addition of LYPLA-I/APT1, in contrast to a 1.3-fold increase without LYPLA-I/APT1. Similarly, LPC 20:4 (Fig. 6D) increased 2.8-fold with the addition of LYPLA-I/APT1 and 2.5-fold without LYPLA-I/APT1. In the same samples, LPA 18:2 (Fig. 6A) increased 3.5-fold over 24 h compared with 2.6-fold without LYPLA-I/APT1. LPA 20:4 (Fig. 6B) increased 4.6-fold without the addition of LYPLA-I/APT1 relative to the level found at the beginning of the incubation and 5.8-fold with the addition of LYPLA-I/APT1. The addition of LYPLA-I/APT1 significantly increased the production of polyunsaturated LPC and LPA, indicating that this enzyme

contributes to the production of LPA during blood coagulation.

Regioisomeric preference of ATX

To further understand the mechanism of LPA production upon blood coagulation, we wanted to determine the regioisomeric preference of ATX. We had determined that LYPLA-I/APT1 cleaves phospholipids to yield *sn*-2 LPLs. These LPLs can either undergo acyl migration and then be further cleaved by ATX to yield *sn*-1 LPA or the *sn*-2 LPLs can first be cleaved by ATX yielding *sn*-2 LPA that then undergoes acyl migration to form *sn*-1 LPA. As the *sn*-2 regioisomer of LPC is relatively unstable ($T_{1/2} \sim 30$ min at pH 8.0), especially during incubation at 37°C (31) (acyl migration generates a 9:1 excess of the *sn*-1 form), we were unable to use the natural substrate for ATX to experimentally determine substrate preference. To prevent acyl migration, we used lyso-PAF, an analog of LPC in which the fatty acid is ether-linked to the glycerol backbone. Using an Amplex Red, fluorescence-based choline release assay, we determined the K_m and V_{max} of the *sn*-1 regioisomer to be $96 \pm 10 \mu\text{M}$ and $0.11 \pm 0.003 \mu\text{M}\cdot\text{min}^{-1}$, respectively. In contrast, the K_m and V_{max} of the *sn*-2 regioisomer were $51 \pm 4 \mu\text{M}$ and $0.03 \pm 0.004 \mu\text{M}\cdot\text{min}^{-1}$, respectively (Table 3). The k_{cat} value for the *sn*-1 regioisomer was $11 \pm 0.03 \text{ min}^{-1}$, whereas for the *sn*-2 regioisomer it was $3 \pm 0.14 \text{ min}^{-1}$. The K_m and k_{cat} values help assess the efficiency of the enzymes against a given substrate; however, these values should not be used alone when considering the kinetic parameters of an enzyme. To better compare the enzyme

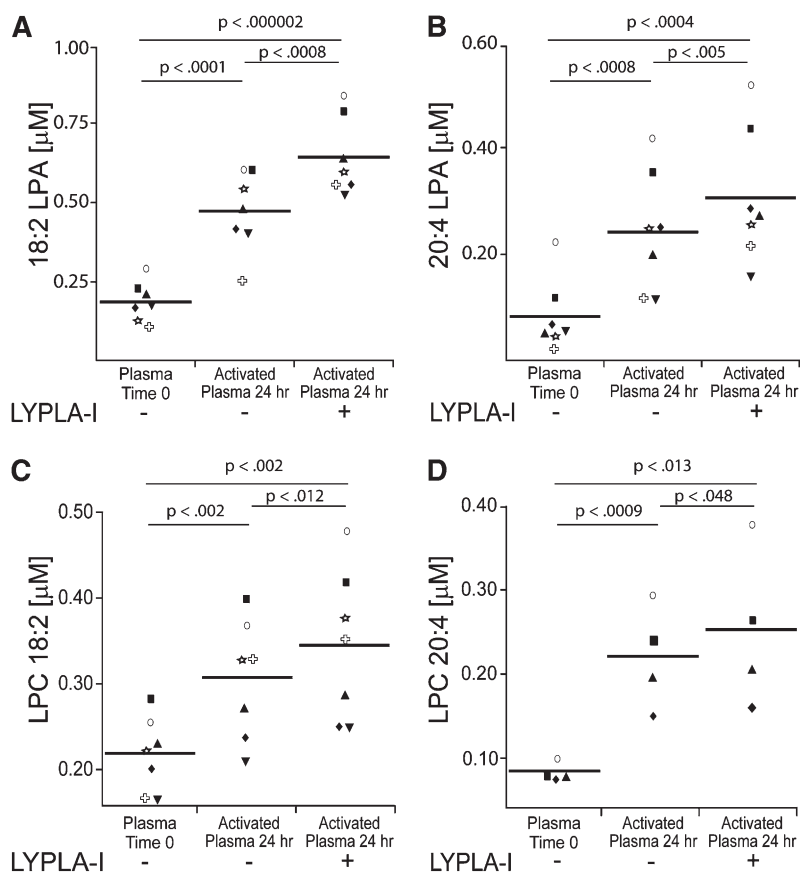


Fig. 6. Human recombinant LYPLA-I/APT1 increases the amount of LPA 18:2 (A), LPA 20:4 (B), LPC 18:2 (C), and LPC 20:4 (D) produced in physiologically activated plasma. Physiologically activated plasma was incubated with or without human recombinant LYPLA-I/APT1 for 24 h. LPA 18:2 and LPA 20:4 increased in 24 h compared to the amount present in plasma immediately after blood draw. Production of LPA and LPC substantially increased with the addition of LYPLA-I/APT1, showing that LYPLA-I/APT1 plays a role in the production of LPA during blood coagulation. Results are from three female donors and four male donors (A-C) or one female donor and three male donors (D). Open symbols represent female donors, and closed symbols represent male donors. Identical shapes throughout indicate same donor. $P < 0.05$, 24 h activated plasma with LYPLA-I versus without LYPLA-I analyzed by paired *t*-test.

efficiency for the two substrates, the ratio k_{cat}/K_m (specificity constant) can be used. The constant provides a measure of catalytic efficiency and allows for direct comparison of the efficiency of an enzyme toward different substrates. The k_{cat}/K_m values for the *sn-1* and *sn-2* regioisomers of lyso-PAF 18:1 were $0.12 \pm 0.01 \mu\text{M}^{-1}\cdot\text{min}^{-1}$ and $0.05 \pm 0.01 \mu\text{M}^{-1}\cdot\text{min}^{-1}$, respectively (Fig. 7). Thus, the K_{cat}/K_m of the *sn-1* regioisomer was 2.3 times higher than that of the *sn-2* regioisomer, indicating that ATX catalyzes the *sn-1* regioisomer of lyso-PAF 18:1 more efficiently than the *sn-2* regioisomer.

DISCUSSION

We identified LYPLA-I/APTI as an enzyme with PLA₁ activity that is released from human platelets during blood clotting and that contributes to the generation of polyunsaturated species of LPA abundant in serum. Since the early reports of Schumacher et al. and Mauco et al. (16, 21) in the late seventies, it has been known that platelet activation and LPA production were coupled; however, the precise mechanism remained unknown (17–20). Previously we have shown that only trace amounts of LPA are generated in activated platelets, far less than could account for the rise in LPA concentration from the nanomolar range in plasma to the several micromolar level found in serum (19). Attention in the field has since been focused on the hypothesis that activated platelets release phospholipases, which generate a new pool of LPLs that is subsequently converted to LPA by ATX (19, 39). Because more than 80% of LPA in serum is composed of the polyunsaturated 18:2 and 20:4 acyl species, we proposed that the LPL pool accessed by the constitutive ATX in plasma is likely to be generated by PLA₁ enzyme(s) derived from activated platelets (19). In pursuit of this hypothesis, we report in this study the identification of one such PLA₁ enzyme, previously known as LYPLA-I/APTI, which contributes to the increase in LPA production during blood coagulation. Even though our results suggest that this PLA₁ is a major contributor to the increase in LPA production, it may not be the only contributing phospholipase released by activated human platelets.

Previous studies have used fluorescent phospholipids or [³²P]orthophosphate for biosynthetic labeling of the substrates to monitor platelet-derived phospholipases (19). We developed LC-MS/MS techniques to monitor the sequential cleavage of PC/PS to LPC/LPS to LPA without the use of unnatural, fluorescently labeled substrates. Sano et al. showed that when fluorescently labeled PC, PE, or PS was incubated with supernatant from thrombin-stimulated platelets no LPA production could be detected. However, when plasma or serum was added, LPA generation commenced, suggesting that elements of the biochemical

pathway were missing from the platelet supernatant (19). Using our newly developed method, we were able to directly demonstrate that ATX addition to platelet supernatant significantly increased LPA production, indicating that there was de novo generation of ATX substrates within the platelet supernatant (Fig. 1). Using *sn-2* NBD-labeled PC and PS, we found overwhelming hydrolytic activity generating NBD-LPC/LPS, consistent with the abundant presence of PLA₁ activity in the platelet supernatant. Under these conditions, we found much less NBD-FA generation from either NBD-labeled phospholipid substrate, indicating that PLA₂ activity was lower than corresponding PLA₁ activity toward these substrates. In the absence of exogenously added recombinant ATX, more LPA (although very little) was generated from PS than from PC. This finding might indicate that some lysophospholipase D enzymes present in the supernatant prefer LPS over LPC, or that trace amounts of contaminating ATX from plasma was present in the supernatant. It is also possible that the NBD-labeled lipids are poor substrates for ATX but good substrates for LYPLA-I. Lastly, it is known that LYPLA-I/APTI is a multifunctional enzyme that cleaves LPC as a lysophospholipase and PC as a phospholipase. The lysophospholipase activity could have consumed LPC more readily than LPS, diminishing the former substrate from ATX and thereby decreasing the amount of LPA produced.

Pamuklar et al. (40) examined the interaction of ATX with β_3 integrin expressed on platelets and proposed that this mechanism could localize and augment LPA production at the surface of platelets. We did not detect substantial LPA production by activated purified human platelets in the absence of added ATX (Fig. 1). Thus, it appears that little ATX is associated with nonactivated circulating human platelets and activation of β_3 integrins is required for capturing ATX to the platelet surface. Whether LPA receptors expressed in platelets activate β_3 integrins, thereby promoting ATX binding, remains to be demonstrated. Such a feed-forward mechanism amplifying LPA production at the platelet surface and promoting platelet activation via LPA receptors could play a role in thrombosis and hemostasis.

Using three sequential chromatographic steps, we were unable to purify the PLA₁ activity to homogeneity. We pursued an affinity-labeling strategy using an FP probe, which selectively reacted with serine residues in the catalytic site of serine hydrolases to which most lipases belong (36). Using the FP-biotin-labeled serine hydrolases isolated from the partially purified PLA₁ fraction, we applied LC-MS/MS in combination with database searches to identify these enzymes. We searched for proteins that were known lipases among FP-biotin-labeled proteins. Most lipase domain members have characteristic surface loops (β_9 loops)

TABLE 3. Kinetic parameters for ATX-mediated hydrolysis of Lyso-PAF 18:1

Lyso-PAF	K_m (μM)	V_{max} ($\mu\text{M}\cdot\text{min}^{-1}$)	K_{cat} (min^{-1})	K_{cat}/K_m ($\mu\text{M}^{-1}\cdot\text{min}^{-1}$)
<i>sn-1</i>	96 ± 10	0.11 ± 0.003	11 ± 0.03	0.12 ± 0.01
<i>sn-2</i>	51 ± 4	0.025 ± 0.004	3.0 ± 0.1	0.050 ± 0.01

N = 3, average values \pm SE.

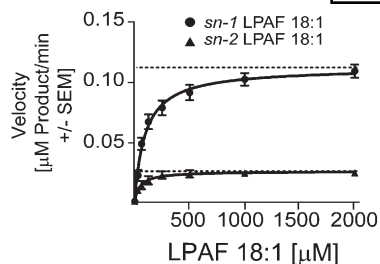


Fig. 7. Comparison of the cleavage of *sn-1* with *sn-2* lyso-PAF 18:1 by ATX. A linear segment of time versus amount of product was plotted for each substrate concentration (31.25 μ M–2 mM) to determine initial velocity. Substrate concentration versus initial velocity was plotted. All absorbance values were converted to μ M of resorufin produced to report as actual product. Bars are the mean of three independent determinations \pm SEM.

and a lid domain (12). These loops are part of the active site and help determine substrate recognition. The domains helped to identify our protein of interest. We also ignored all proteins that were too large to fit the size of the PLA₁ estimated by gel filtration (25 kDa and 50 kDa; data not shown) and excluded any unknown peptide sequences. Using these exclusion criteria, we identified four proteins that were potential candidates for a PLA₁. We further reasoned that if PLA₁ is released from platelets, it should be synthesized in platelets. Therefore, we looked for RNA transcripts of the four lipases in platelets. Using this criterion, we were able to eliminate LCAT and PS-PLA₁, leaving MGLL and LYPLA-I/APT1 as the two candidates.

We were also able to eliminate MGLL as a candidate protein because the recombinant enzyme lacked PLA₁ activity. We next cloned and expressed the human LYPLA-I/APT1 and unexpectedly found that the GST tag interfered with enzymatic activity. We do not know whether the GST tag may have interfered with protein folding or may have affected the ability of the substrate to bind to the enzyme. Despite this interference, once the GST tag was removed, we determined that the recombinant LYPLA-I/APT1 had PLA₁ activity against NBD-labeled and natural PC and PS. Our attempts to determine the K_m value of LYPLA-I/APT1 with PC and PS substrates were unsuccessful because the product of PLA₁ cleavage is also the substrate of the lysophospholipase activity of the enzyme. LYPLA-I/APT1 has been shown to cleave fatty acids esterified to either the *sn-1* or the *sn-2* carbon of LPC (41). However, we determined that LPA was not cleaved by LYPLA-I/APT1, indicating that the product escapes further modification by this multifunctional enzyme.

Another function of LYPLA-I/APT1 is the deacylation/depalmitoylation of G proteins, ghrelin, and other thioacylated protein substrates (38, 42–44). Deacylation/depalmitoylation contributes to the regulation of lipid modifications and reverses the process of thioacylation of proteins involved in signal transduction. It has been shown that the K_m of the lysophospholipase activity is about 8 times higher than the K_m of the thioesterase activity of the enzyme. The V_{max} is about 17 times lower for the lysophospholipase activity than for the thioesterase activity (44).


On the basis of these data, it has been proposed that LYPLA-I/APT1 has a much higher thioesterase activity than lysophospholipase activity. However, *in vivo*, the activity of this enzyme is likely to be affected by the availability and presentation of the different substrates.

To make a distinction between substrate preference for PC and LPC of LYPLA-I/APT1, we used NBD-PC substrate and followed the time course of NBD-LPC production generated by the PLA₁ activity and NBD-FA production generated through lysophospholipase activity. We observed a considerable delay in the formation of NBD-FA relative to NBD-LPC, the latter being continuously generated. For this reason, we suggest that LYPLA-I/APT1 functions preferentially as a PLA₁ and only after the buildup of LPL concentration, presumably via acyl migration, it begins to cleave this substrate as a lyso-PLA₁. Although LYPLA-I/APT1 also may be able to function as a PLA₂, its PLA₁ activity accounts for the generation of polyunsaturated LPA, whereas the PLA₂ activity would generate LPL molecular species overwhelmingly of the saturated type. In this context, we emphasize that ATX present in blood will cleave the headgroups of the nascent LPL generated by LYPLA-I/APT1. Once the headgroup is removed, the LPA is no longer cleaved by LYPLA-I/APT1 (Fig. 4B), allowing for the accumulation of LPA in serum.

Without a knockout animal model or specific inhibitors of LYPLA-I/APT1, we were limited to study the effect of the enzyme on *ex vivo* LPA production in activated plasma. Following the addition of LYPLA-I/APT1 to heparinized plasma, we detected only a very small increase in polyunsaturated LPA production at 24 h, suggesting that the enzyme can utilize physiological substrates. However, this increase was confounded because heparin inhibited the activity of ATX but not the PLA₁ activity of LYPLA-I/APT1. LPA production in activated plasma began to increase after 3 h and continued up to 24 h (the last time point tested). Spiking LYPLA-I/APT1 into activated nonanticoagulated plasma increased LPA 18:2 and 20:4 production by 5- and 4-fold, respectively. This augmentation of LPA production indicates that LYPLA-I/APT1 recognizes and cleaves plasma phospholipids and contributes to the generation of LPA during blood coagulation. Production of LPA by this pathway is limited by the amount of LYPLA-I/APT1 released from platelets and the rate with which ATX generates LPA relative to the rate with which LYPLA-I/APT1 degrades LPL.

We considered that LYPLA-I/APT1 generates a new pool of *sn-2* LPL, which can potentially undergo acyl migration before or after headgroup cleavage by ATX. The *sn-2* regioisomer of LPC is relatively unstable and undergoes acyl migration to the *sn-1* position at neutral pH at 37°C. Due to the several minute-long half-life of the *sn-2* regioisomer (31), we were unable to obtain biochemical proof whether the nascent LPA generated was of the *sn-2* or *sn-1* regioisomer because the extraction and HPLC separation of the regioisomers takes longer than 30 min. To obtain indirect insight into the role of acyl migration on ATX cleavage, we synthesized the *sn-2* regioisomer of lyso-PAF and compared its cleavage with the *sn-1* regioisomer. ATX cleaved the *sn-1* lyso-PAF with a higher k_{cat}/K_m than

its *sn-2* counterpart. Based on this finding, it seems logical to propose that acyl migration occurs predominantly at the LPL stage of this biochemical pathway. However, only direct measurement of the nascent LPL and LPA regioisomers can help settle this question. An additional factor that must be considered is the short half-life of LPA in blood in vivo. LPA appears to be continuously produced and simultaneously broken down in blood on the minute scale (45). This might create a situation that could enrich the abundance of *sn-2* regioisomer in blood relative to the *sn-1* regioisomer because the LPA generated is broken down before or at a similar rate with which acyl migration occurs.

On the basis of the results of this study, we hypothesize that LPA production during blood coagulation occurs via the following steps: 1) Upon activation, platelets release LYPLA-I/APT1; 2) LYPLA-I/APT1 cleaves phospholipids to generate a new pool of *sn-2* LPL; 3) The newly generated *sn-2* LPLs undergo acyl migration within minutes to produce a pool of *sn-1* LPLs; and 4) ATX or other lysophospholipase D enzymes cleave the *sn-1* LPLs to generate an upsurge of *sn-1* LPA enriched in polyunsaturated FA. This hypothesis needs further testing. The availability of LYPLA-I/APT1 knockout animals and rapid methods for the detection of LPA and LPA regioisomers will accelerate the progress toward a better understanding of LPA production in biological fluids. 

The authors thank Prof. Akira Tokumura (University of Tokushima) for his help with the LC-MS protocol.

REFERENCES

1. Tigyi, G. 2010. Aiming drug discovery at lysophosphatidic acid targets. *Br. J. Pharmacol.* **161**: 241–270.
2. Mills, G. B., and W. H. Moolenaar. 2003. The emerging role of lysophosphatidic acid in cancer. *Nat. Rev. Cancer.* **3**: 582–591.
3. Tigyi, G., and A. L. Parrill. 2003. Molecular mechanisms of lysophosphatidic acid action. *Prog. Lipid Res.* **42**: 498–526.
4. Pages, C., M. F. Simon, P. Valet, and J. S. Saulnier-Blache. 2001. Lysophosphatidic acid synthesis and release. *Prostaglandins Other Lipid Mediat.* **64**: 1–10.
5. Tsukahara, T., R. Tsukahara, Y. Fujiwara, J. Yue, Y. Cheng, H. Guo, A. Bolen, C. Zhang, L. Balazs, F. Re, et al. 2010. Phospholipase D2-dependent inhibition of the nuclear hormone receptor PPARgamma by cyclic phosphatidic acid. *Mol. Cell.* **39**: 421–432.
6. Gendaszewska-Darmach, E. 2008. Lysophosphatidic acids, cyclic phosphatidic acids and autotaxin as promising targets in therapies of cancer and other diseases. *Acta Biochim. Pol.* **55**: 227–240.
7. Aoki, J. 2004. Mechanisms of lysophosphatidic acid production. *Semin. Cell Dev. Biol.* **15**: 477–489.
8. Mishra, R. S., K. A. Carnevale, and M. K. Cathcart. 2008. iPLA2beta: front and center in human monocyte chemotaxis to MCP-1. *J. Exp. Med.* **205**: 347–359.
9. Carnevale, K. A., and M. K. Cathcart. 2001. Calcium-independent phospholipase A(2) is required for human monocyte chemotaxis to monocyte chemoattractant protein 1. *J. Immunol.* **167**: 3414–3421.
10. Bektas, M., S. G. Payne, H. Liu, S. Goparaju, S. Milstien, and S. Spiegel. 2005. A novel acylglycerol kinase that produces lysophosphatidic acid modulates cross talk with EGFR in prostate cancer cells. *J. Cell Biol.* **169**: 801–811.
11. Nagai, Y., J. Aoki, T. Sato, K. Amano, Y. Matsuda, H. Arai, and K. Inoue. 1999. An alternative splicing form of phosphatidylserine-specific phospholipase A1 that exhibits lysophosphatidylserine-specific lysophospholipase activity in humans. *J. Biol. Chem.* **274**: 11053–11059.
12. Aoki, J., Y. Nagai, H. Hosono, K. Inoue, and H. Arai. 2002. Structure and function of phosphatidylserine-specific phospholipase A1. *Biochim. Biophys. Acta.* **1582**: 26–32.
13. Fourcade, O., M. F. Simon, C. Viode, N. Rugani, F. Leballe, A. Ragab, B. Fournie, L. Sarda, and H. Chap. 1995. Secretory phospholipase A2 generates the novel lipid mediator lysophosphatidic acid in membrane microvesicles shed from activated cells. *Cell.* **80**: 919–927.
14. Siess, W., K. J. Zangl, M. Essler, M. Bauer, R. Brandl, C. Corrinth, R. Bittman, G. Tigyi, and M. Aepfelbacher. 1999. Lysophosphatidic acid mediates the rapid activation of platelets and endothelial cells by mildly oxidized low density lipoprotein and accumulates in human atherosclerotic lesions. *Proc. Natl. Acad. Sci. USA.* **96**: 6931–6936.
15. Cummings, R., N. Parinandi, L. Wang, P. Usatyuk, and V. Natarajan. 2002. Phospholipase D/phosphatidic acid signal transduction: role and physiological significance in lung. *Mol. Cell. Biochem.* **234–235**: 99–109.
16. Mauco, G., H. Chap, M. F. Simon, and L. Douste-Blazy. 1978. Phosphatidic and lysophosphatidic acid production in phospholipase C-and thrombin-treated platelets. Possible involvement of a platelet lipase. *Biochimie.* **60**: 653–661.
17. Eichholtz, T., K. Jalink, I. Fahrenfort, and W. H. Moolenaar. 1993. The bioactive phospholipid lysophosphatidic acid is released from activated platelets. *Biochem. J.* **291**: 677–680.
18. Gaits, F., O. Fourcade, F. Le Balle, G. Gueguen, B. Gaige, A. Gassama-Diagne, J. Fauvel, J. P. Salles, G. Mueco, M. F. Simon, et al. 1997. Lysophosphatidic acid as a phospholipid mediator: pathways of synthesis. *FEBS Lett.* **410**: 54–58.
19. Sano, T., D. Baker, T. Virag, A. Wada, Y. Yatomi, T. Kobayashi, Y. Igarashi, and G. Tigyi. 2002. Multiple mechanisms linked to platelet activation result in lysophosphatidic acid and sphingosine 1-phosphate generation in blood. *J. Biol. Chem.* **277**: 21197–21206.
20. Aoki, J., A. Inoue, and S. Okudaira. 2008. Two pathways for lysophosphatidic acid production. *Biochim. Biophys. Acta.* **1781**: 513–518.
21. Schumacher, K. A., H. G. Classen, and M. Spath. 1979. Platelet aggregation evoked in vitro and in vivo by phosphatidic acids and lysoderivatives: identity with substances in aged serum (DAS). *Thromb. Haemost.* **42**: 631–640.
22. Tokumura, A., E. Majima, Y. Kariya, K. Tominaga, K. Kogure, K. Yasuda, and K. Fukuzawa. 2002. Identification of human plasma lysophospholipase D, a lysophosphatidic acid-producing enzyme, as autotaxin, a multifunctional phosphodiesterase. *J. Biol. Chem.* **277**: 39436–39442.
23. Umezū-Goto, M., Y. Kishi, A. Taira, K. Hama, N. Dohmae, K. Takio, T. Yamori, G. B. Mills, K. Inoue, J. Aoki, et al. 2002. Autotaxin has lysophospholipase D activity leading to tumor cell growth and motility by lysophosphatidic acid production. *J. Cell Biol.* **158**: 227–233.
24. Baker, D. L., D. M. Desiderio, D. D. Miller, B. Tolley, and G. J. Tigyi. 2001. Direct quantitative analysis of lysophosphatidic acid molecular species by stable isotope dilution electrospray ionization liquid chromatography-mass spectrometry. *Anal. Biochem.* **292**: 287–295.
25. Hosogaya, S., Y. Yatomi, K. Nakamura, R. Ohkawa, S. Okubo, H. Yokota, M. Ohta, H. Yamazaki, T. Koike, and Y. Ozaki. 2008. Measurement of plasma lysophosphatidic acid concentration in healthy subjects: strong correlation with lysophospholipase D activity. *Ann. Clin. Biochem.* **45**: 364–368.
26. van Meeteren, L. A., P. Ruurs, C. Stortelers, P. Bouwman, M. A. van Rooijen, J. P. Pradere, T. R. Pettit, M. J. Wakelam, J. S. Saulnier-Blache, C. L. Mummery, et al. 2006. Autotaxin, a secreted lysophospholipase D, is essential for blood vessel formation during development. *Mol. Cell. Biol.* **26**: 5015–5022.
27. Tanaka, M., S. Okudaira, Y. Kishi, R. Ohkawa, S. Iseki, M. Ota, S. Noji, Y. Yatomi, J. Aoki, and H. Arai. 2006. Autotaxin stabilizes blood vessels and is required for embryonic vasculature by producing lysophosphatidic acid. *J. Biol. Chem.* **281**: 25822–25830.
28. Fujiwara, Y., V. Sardar, A. Tokumura, D. Baker, K. Murakami-Murofushi, A. Parrill, and G. Tigyi. 2005. Identification of residues responsible for ligand recognition and regioisomeric selectivity of lysophosphatidic acid receptors expressed in mammalian cells. *J. Biol. Chem.* **280**: 35038–35050.
29. Bandoh, K., J. Aoki, A. Taira, M. Tsujimoto, H. Arai, and K. Inoue. 2000. Lysophosphatidic acid (LPA) receptors of the EDG family are differentially activated by LPA species. Structure-activity relationship of cloned LPA receptors. *FEBS Lett.* **478**: 159–165.
30. Yanagida, K., K. Masago, H. Nakanishi, Y. Kihara, F. Hamano, Y. Tajima, R. Taguchi, T. Shimizu, and S. Ishii. 2009. Identification

- and characterization of a novel lysophosphatidic acid receptor, p2y5/LPA6. *J. Biol. Chem.* **284**: 17731–17741.
31. Pluckthun, A., and E. A. Dennis. 1982. Acyl and phosphoryl migration in lysophospholipids: importance in phospholipid synthesis and phospholipase specificity. *Biochemistry.* **21**: 1743–1750.
32. Tokumura, A., L. D. Carbone, Y. Yoshioka, J. Morishige, M. Kikuchi, A. Postlethwaite, and M. A. Watsky. 2009. Elevated serum levels of arachidonoyl-lysophosphatidic acid and sphingosine 1-phosphate in systemic sclerosis. *Int. J. Med. Sci.* **6**: 168–176.
33. Tokumura, A., K. Harada, K. Fukuzawa, and H. Tsukatani. 1986. Involvement of lysophospholipase D in the production of lysophosphatidic acid in rat plasma. *Biochim. Biophys. Acta.* **875**: 31–38.
34. Tokumura, A., M. Miyake, O. Yoshimoto, M. Shimizu, and K. Fukuzawa. 1998. Metal-ion stimulation and inhibition of lysophospholipase D which generates bioactive lysophosphatidic acid in rat plasma. *Lipids.* **33**: 1009–1015.
35. Tokumura, A., S. Yamano, T. Aono, and K. Fukuzawa. 2000. Lysophosphatidic acids produced by lysophospholipase D in mammalian serum and body fluid. *Ann. N. Y. Acad. Sci.* **905**: 347–350.
36. Leung, D., C. Hardouin, D. L. Boger, and B. F. Cravatt. 2003. Discovering potent and selective reversible inhibitors of enzymes in complex proteomes. *Nat. Biotechnol.* **21**: 687–691.
37. Liu, Y., M. P. Patricelli, and B. F. Cravatt. 1999. Activity-based protein profiling: the serine hydrolases. *Proc. Natl. Acad. Sci. USA.* **96**: 14694–14699.
38. Duncan, J. A., and A. G. Gilman. 1998. A cytoplasmic acyl-protein thioesterase that removes palmitate from G protein alpha subunits and p21(RAS). *J. Biol. Chem.* **273**: 15830–15837.
39. Aoki, J., A. Taira, Y. Takanezawa, Y. Kishi, K. Hama, T. Kishimoto, K. Mizuno, K. Saku, R. Taguchi, and H. Arai. 2002. Serum lysophosphatidic acid is produced through diverse phospholipase pathways. *J. Biol. Chem.* **277**: 48737–48744.
40. Pamuklar, Z., L. Federico, S. Liu, M. Umezū-Goto, A. Dong, M. Panchatcharam, Z. Fulerson, E. Berdyshev, V. Natarajan, X. Fang, et al. 2009. Autotaxin/lysopholipase D and lysophosphatidic acid regulate murine hemostasis and thrombosis. *J. Biol. Chem.* **284**: 7385–7394.
41. Wang, A., R. Loo, Z. Chen, and E. A. Dennis. 1997. Regiospecificity and catalytic triad of lysophospholipase I. *J. Biol. Chem.* **272**: 22030–22036.
42. Duncan, J. A., and A. G. Gilman. 2002. Characterization of *Saccharomyces cerevisiae* acyl-protein thioesterase 1, the enzyme responsible for G protein alpha subunit deacylation in vivo. *J. Biol. Chem.* **277**: 31740–31752.
43. Satou, M., Y. Nishi, J. Yoh, Y. Hattori, and H. Sugimoto. 2010. Identification and characterization of acyl-protein thioesterase 1/lysophospholipase I as a ghrelin deacylation/lysophospholipid hydrolyzing enzyme in fetal bovine serum and conditioned medium. *Endocrinology.* **151**: 4765–4775.
44. Hirano, T., M. Kishi, H. Sugimoto, R. Taguchi, H. Obinata, N. Ohshima, K. Tatei, and T. Izumi. 2009. Thioesterase activity and subcellular localization of acylprotein thioesterase 1/lysophospholipase I. *Biochim. Biophys. Acta.* **1791**: 797–805.
45. Albers, H. M., A. Dong, L. A. van Meeteren, D. A. Egan, M. Sunkara, E. W. van Tilburg, K. Schuurman, O. van Tellingen, A. J. Morris, S. S. Smyth, et al. 2010. Boronic acid-based inhibitor of autotaxin reveals rapid turnover of LPA in the circulation. *Proc. Natl. Acad. Sci. USA.* **107**: 7257–7262.